

# Obtaining Composite Materials of Sulphonated Polystyrene (PSS) – Bi-Sn

Helia Bibiana León-Molina <sup>a\*</sup>, Oscar Suarez <sup>b</sup>

a Universidad ECCI, Grupo de Investigación GIDMyM, Bogotá, Colombia

b Universidad Nacional de Colombia, Dpto Ing Sistemas e Industrial, Bogotá, Colombia

[hleonm@ecc.edu.co](mailto:hleonm@ecc.edu.co)

Copolymer - metal composites are very interesting materials for engineering applications, as they offer tailored properties from the composing materials, such as flexibility, low density, conductivity, among others. Sulfonated polystyrene was synthesized by emulsion polymerization in an aqueous medium using Brij (polyoxyethylene 23 dodecyl ether) as surfactant. The composite material was obtained through the reduction of the metallic salt ( $\text{BiCl}_3$  or  $\text{SnCl}_2$ ) in a solution of dimethylformamide and the copolymer, and Brij as stabilizers. Scanning electron microscopy images evidenced evenly distributed particles of metal. Isolated particles were observed in the case of Tin, while Bismuth showed bunches, as reported in previous publications. Differential scanning calorimetry tests depicted the expected behavior of  $T_g$  for the sulphonated polystyrene with small variations in the composites. A peak for the melting point around 232 °C was observed for tin, while the system Polymer-Bi had no evidence of bismuth melting point, these differences could be related to bismuth crystal size.

## 1. Introduction

Tin and Bismuth are friendly heavy metals with special properties in their metallic and oxide state. Tin has gained attention due to its optoelectronic and electrochemical properties (Hörmann et al., 2015), as anode tin has higher capacity than graphite electrodes (Wei Ni, Jianli Cheng, 2012), while in its oxide state it is a semiconductor with high capacitance. These properties are ideal for example in long life and powerful batteries. Metallic bismuth has been used for detection of heavy metals by electrochemical methods (Serrano et al., 2008; Suarez et al., 2018) also as absorber of high energy X-rays for astrophysics applications (Ferruggia Bonura et al., 2020). Bismuth oxides can present photocatalytic activity (Lai et al., 2019) and other electronic properties (Devi & Ray, 2020).

Composite materials are formed when two or more materials or phases of a material come together to provide a new combination of properties that are not possible otherwise. Composite materials can be selected for obtaining unusual combinations of stiffness, weight, thermal resistance, chemical activity or conductivity. These materials reveal the way different materials can work synergistically. Polymer - metal composites are very interesting materials for engineering applications, as they offer tailored properties from the composing materials, such as flexibility, low density, conductivity, among others. For these reasons, new devices and sensors have been developed based on composites or nanostructured metal-polymer systems (Peponi et al., 2014; Shrivastava et al., 2016).

The properties of composites depend not only on the properties of their individual components but also on the morphology and interactions between phases. Significant efforts have been made to achieve control of nanostructures using various approaches. For example, by creating nanoparticles it is possible to control some fundamental properties such as melting temperature, magnetic behaviour, charge capacity, electrochemical potential and even colour without changing the chemical composition.

The stabilization mechanisms of nanoparticles can be classified into electrostatic, steric, or a combination of both. The first is based on the separation of electric charges due to the formation of a double electrical layer around the particles, while the second is based on geometric and spatial repulsion due to the large size of the adsorbed molecules on the nanoparticle surface (Kraynov & Müller, 2011).

The high adsorption energy of the polymer chains is attributed to the high values of the van Der Waals interaction between the surface and the many repeating units of the polymer chain. The total energy of adsorption per molecule must be compensated by the loss of configurational entropy of the adsorbed polymer. In some cases, homopolymers can be adsorbed through a specific interaction, for example, hydrogen bonds in the case of polyethylene oxides or polyvinyl pyrrolidone on silica or bismuth nanoparticles (Reverberi et al., 2019). As long as no ionic charges are involved, these surfactant polymers can be used in presence of high concentration electrolytes and high temperatures (Rozenberg & Tenne, 2008). The idea of employing a voluminous adsorbent and highly charged polymer for the stabilization of nanoparticles results in the so-called electrosteric stabilization.

Poly sodium 4-styrenesulfonate (PSS) is a polyelectrolyte that can be used as support of proteins or nanoparticles due to its configuration (Sandra et al., 2005). Theoretical calculations have shown that the PSS structure can change its configuration to a cylinder, semicircle or torus when ionic strength changes from  $10^{-3}$  to  $10^{-1}$  M in presence of water molecules (Adamczyk et al., 2009). These configurations have an effective length in the order of 10 nm, which is enough to encapsulate, for example, metallic nanoparticles.

In previous work we used PSS in addition with styrene and divinyl benzene as a thermoset matrix for metallic nanoparticles (Suarez, 2017). In this work we opted for synthesized and studied the thermal and structural behavior of PSS-Bi and PSS-Sn composites as a first step for further possible applications in electrochemical or optoelectronic fields, where the polymer matrix not only stabilize the particles but also facilitate the manufacture of devices through plastic shaping processes.

## 2. Experimental

### 2.1 Polymer synthesis

Copolymers of styrene (Aldrich), and vinyl benzene sodium sulfonate-VBS (Aldrich) were produced in a three-necked flask by emulsion polymerization at 80°C under stirring for 2 hours as in the protocol reported by (Suarez, 2017). The VBS (12 to 30% by weight) was added after 30 min of styrene reaction. Polyoxyethylene dodecyl ether - brij L23 (Aldrich) was used as surfactant for polymerization at 0.075% in water. Potassium persulfate was used as initiator with a concentration of 0.55% with respect to the monomers weight. The composition of any reactive mix for polymer synthesis is presented in Table 1.

*Table 1: Composition of sulfonated copolymers.*

Copolymer	% Styrene	% VBS
P1	87.5	12.5
P2	81.8	18.2
P3	75.7	24.3

### 2.2 Metal nanoparticle synthesis

Solutions of precursors were prepared as reported by (Suarez, 2017) using N-N dimethylformamide-DMF (Aldrich) as solvent; (i) sulfonated copolymer 10 % w/v and (2) the nonionic surfactant brij (Aldrich) 0.9 %w/v as stabilizers; (iii) bismuth chloride (Aldrich) or tin chloride (Merck) at a concentration of 60 mM as metal precursor, and (iv) sodium borohydride (Baker) at a concentration of 320 mM as reductor. The quantities of each solution were calculated to obtain a composition as follows: total metal around 15 mM, brij 0.45% and polymer 5% w/v. After the reduction reaction, cast films of composites were produced and dried at 60 °C in a forced convection oven for later characterization.

### 2.3 Nanocomposite characterization

Differential scanning calorimetry (DSC) was performed in a TAQ10 calorimeter using sealed aluminium capsules, then, samples were weighed in quantities close to 10 mg. The heating program consisted in a previous stage to erase the thermal history of the material as follows: stabilization at 25°C for 1 min; ramp from 20°C/min up to 150 °C for copolymers and up to 300°C for composites; stabilization at the maximum temperature for 1 min, and ramp from 20°C/min up to 25°C. Finally, a ramp from 10°C/min up to the maximum temperature was recorded to analyse the glass transition temperature  $T_g$  and the melting temperature for metal particles  $T_m$ . All runs were made in presence of nitrogen at 50 ml/min.

The morphology of the selected nanocomposite films was observed via scanning electronic microscopy (SEM) in a Phenom Pro X. Samples were coated previously with a thin film of gold in a Cressington sputter coater. The structural characterization was carried out by infrared spectroscopy (FTIR) in a Bruker model alpha 1 spectrometer. The films were directly analysed without previous preparation using ATR mode, and spectrums were recorded in the 400 to 4000  $\text{cm}^{-1}$  range.

### 3. Results

#### 3.1 Structural characterization and thermal behavior

Figure 1 shows the characteristic IR spectra for some of the materials produced. In the case of the copolymers shown in Figure 1 a, special attention should be paid to the bands close to  $3429\text{ cm}^{-1}$ , which correspond to -OH groups. The appearance of this band indicates that the sulphonate groups ( $\text{R-SO}_2\text{O}^-$ ) have exchanged the original sodium atom of the monomer and are in the acidic form in the polymer. The characteristic bands for aromatic rings can also be observed close to  $1436\text{ cm}^{-1}$ . At low wavenumbers, there are other characteristic bands including possible vibrations of the S=O bonds close to  $1200\text{ cm}^{-1}$ .

In the case of composites, the Figure 1 b shows the representative case for the polymer 3 with bismuth and tin. A shift of the OH band is observed in presence of metallic particles. Other works have reported interaction of metallic particles as copper with the polymer matrix (Maldonado, K. Luna, 2017). Likewise, for Tin and bismuth composites in nafion some shifts were observed in the zone of S=O bonds (Suarez et al., 2018). These displacements may be result of the interaction of the electronic cloud of metallic particles with the more electronegative atoms of the polymer chain.

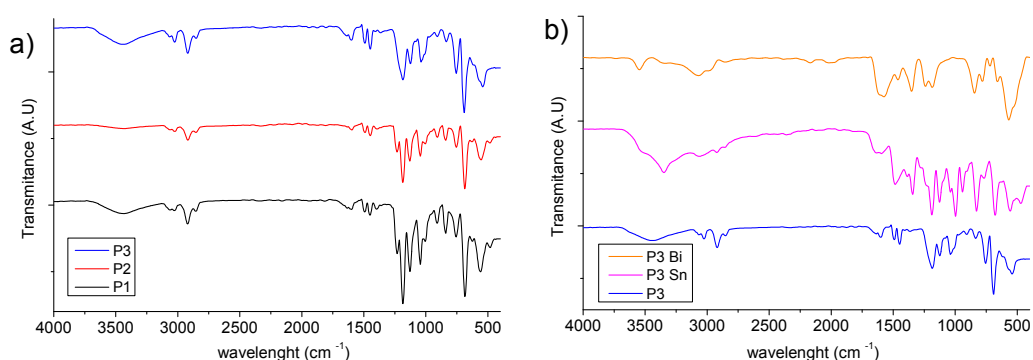


Figure 1: IR spectra of (a) copolymers, and (b) selected composites.

Thermal behaviour of copolymers and composites was studied via DSC. The Figure 2 a shows the glass transition temperature for pure copolymers. It can be observed that the  $T_g$  of the P1 is close to  $100^\circ\text{C}$ . This copolymer corresponds to the one with the lowest content of sulfonate monomer and its  $T_g$  is almost that of pure polystyrene reported above  $100^\circ\text{C}$ . The increase in the content of the sulfonated monomer results in a decrease in  $T_g$  (almost  $10^\circ\text{C}$  for P3), which may indicate that the inclusion of the  $-\text{SO}_2\text{O}-$  groups facilitates the movement of the polymer chains due to the thermal effect.

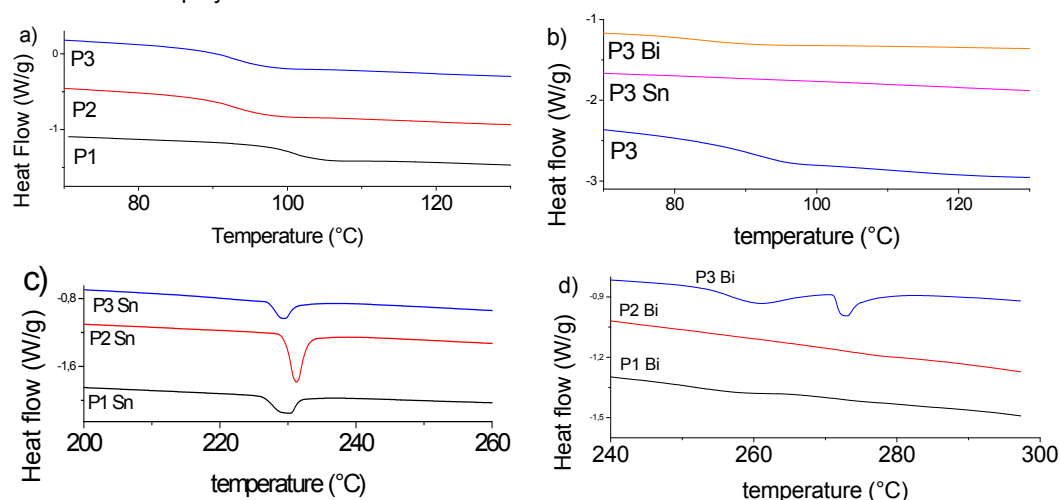


Figure 2: DSC measurements of polymers and selected composites: (a) pure polymers in the  $T_g$  zone; (b) P3 composites in the  $T_g$  zone; (c) polymer-tin composites in  $T_m$  zone and (d) polymer-bismuth composites in  $T_m$  zone.

The glass transition temperature zone for composites produced with different polymers was very different between them, for example, the P3 composites shown in Figure 2b. Although the glass transition zone could not be clearly observed as in the pure polymers, it was possible to observe a slight decrease in P3-Bi, possibly due to the presence of the non-ionic surfactant that would act as plasticizer. The decrease in  $T_g$  allows these materials to be transformed at lower temperatures avoiding possible degradation.

The melting temperature for metallic particles immersed in the polymer matrix is presented in Figure 2c and Figure 2d. The shape and position of metal melting peaks in DSC analysis can change if the particle sizes change as reported in the case of tin-copper nanoparticles (Jo et al., 2011). For P2-Sn composite, a sharp peak was recorded close to 232 °C, which corresponds to the theoretical melting temperature of tin, whilst for P1-Sn and P3-Sn, a wider peak was observed and a slightly lower temperature.

Bismuth has a theoretical melting temperature of 271.4 °C. Although the metal phase was in a similar molar proportion in all composites and the heats of fusion of both tin and bismuth are also similar (7.03 kJ/mol for tin and 11.3 kJ/mol for bismuth), only the P3-Bi composite evidenced a fusion peak. In fact, a wide peak was observed below 271 °C and a sharper one near that value. For P1 and P3 bismuth composites no melting peak was observed. The differences observed with respect to the theoretical temperatures could indicate that the size distributions are different in each material.

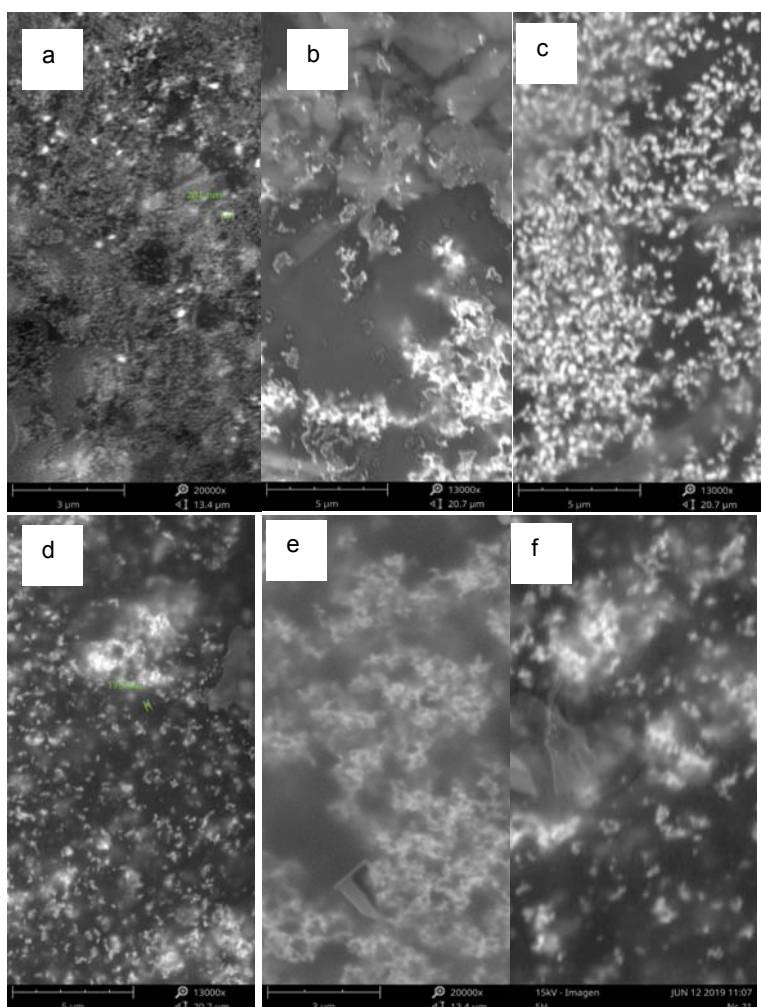


Figure 3: Morphology of PSS-Sn composites: (a) P1-Sn; (b) P2-Sn; (c) P3-Sn; (d) P1-Bi; (e) P2-Bi, and (f) P3-Bi.

### 3.2 Morphology and metal distribution

Figure 3 shows the morphology of the copolymer metal composites. In some cases, rough and even cracked surfaces were observed (not shown) since the polystyrene is a brittle material and is the major component. In the case of tin composites (Figure 3 a - c), discrete particles are observed distributed in a more or less uniform way. EDX analysis showed that bright particles correspond to a phase rich in tin, with a metal content between

20 and 30% approximately. Other elements detected were: C, S and O that are part of the polymer chain. The oxygen content was higher than expected, which suggest that part of the exposed tin was oxidized.

Composites of bismuth appear in Figure 3 d-f. A slight difference was observed in the distribution of the metallic phase, since there is an agglomeration to form clusters. Anyway, Figure 4 confirms that the clusters are formed by discrete particles with smaller sizes. EDX analysis for bismuth composites also shows rich metal phase in brightest regions with a content of 20% Bi, approximately.

Figure 4 a and b, at 60000x shows details of the dispersion of metallic particles in the copolymer. Isolated particles can be observed for tin and cluster for bismuth. The ImageJ software was used for estimating particle size distribution, as shown in the same figure. Similar distributions were obtained for samples of polymer-metal composites taken from different parts. The mean size of the tin particles was in the order of 220 nm with a standard deviation of  $\pm 60$  nm, while for the bismuth particles the mean size was close to the 130 nm  $\pm 30$  nm. The smaller value of size for the bismuth particles could explain the absence of the fusion peak in DSC assays.

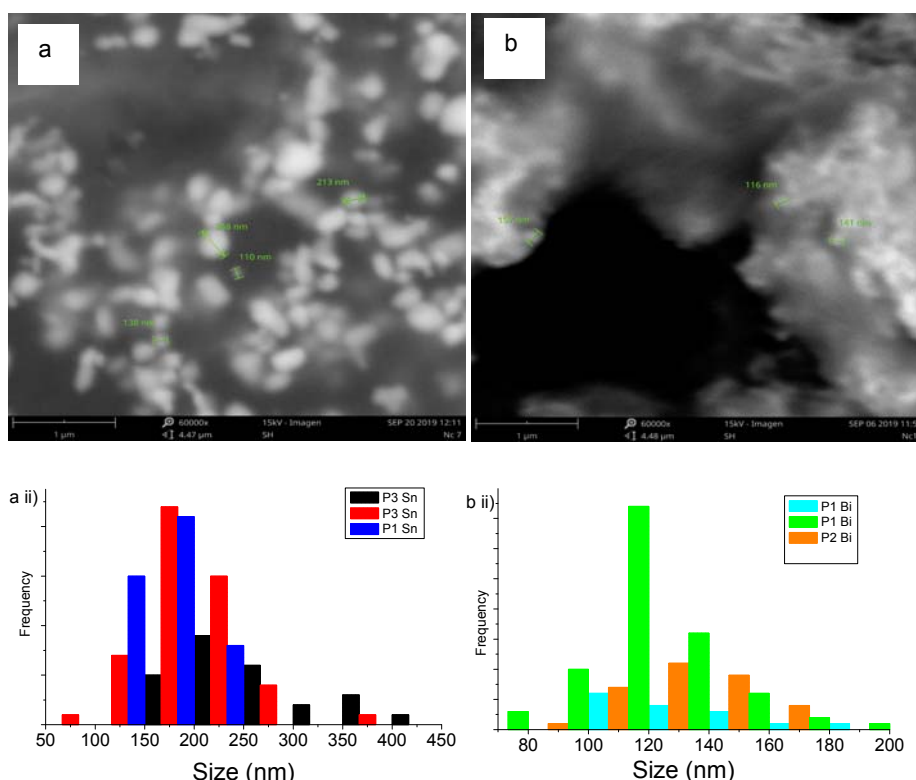


Figure 4: SEM image and particle size distribution of: (a) P3-Sn/P1-Sn and (b) P1-Bi/P2-Bi

#### 4. Conclusions

Sulfonated composites were synthesized and employed as a matrix for tin and bismuth nanoparticles as observed by electronic microscopy. Structural characterization using infrared spectroscopy allowed to observe a possible interaction between the polymer chain and the metal particles due to a shift in the band close to  $3429\text{ cm}^{-1}$  that correspond to the -OH group present in the acidic form of  $\text{R-SO}_2\text{O}^-$  in the polymer.

A decrease in the  $T_g$  of almost  $10^\circ\text{C}$  was observed for the copolymers with the highest content of sulfonated monomer, and possibly another decrease in the composites due to the surfactant used as a nanoparticle stabilization assistant. This decrease possibly facilitates processing of these materials at lower temperatures.

Slight differences were observed between the theoretical melting temperatures of the tin particles and considerable differences in those of bismuth.

SEM analysis and particle size distribution showed that the tin particles were isolated but larger than the bismuth particles that were agglomerated. Mean size of tin particles was around  $220 \pm 60$  nm, while bismuth particles were close to  $130 \pm 30$  nm.

Further research will be done to study the application possibilities of these materials taking advantage of their thermal properties.

## Acknowledgments

Universidad ECCI-Universidad Nacional de Colombia-Universidad Militar Nueva Granada

## References

- Adamczyk, Z., Jachimska, B., Jasiński, T., Warszyński, P., & Wasilewska, M. (2009). Structure of poly (sodium 4-styrenesulfonate) (PSS) in electrolyte solutions: Theoretical modeling and measurements. *Colloids and Surfaces A: Physicochemical and Engineering Aspects*, 343(1–3), 96–103. <https://doi.org/10.1016/j.colsurfa.2009.01.035>
- Devi, N., & Ray, S. S. (2020). Performance of bismuth-based materials for supercapacitor applications: A review. *Materials Today Communications*, 25(September), 101691. <https://doi.org/10.1016/j.mtcomm.2020.101691>
- Ferruggia Bonura, S., Gulli, D., Barbera, M., Collura, A., Spoto, D., Vassallo, P., Varisco, S., Santamaria, M., Di Franco, F., Zaffora, A., Botta, L., & Lo Cicero, U. (2020). Fabrication of Bismuth Absorber Arrays for NTD-Ge Hard X-ray Microcalorimeters. *Journal of Low Temperature Physics*, 200(5–6), 336–341. <https://doi.org/10.1007/s10909-020-02475-6>
- Hörmann, N. G., Gross, A., Rohrer, J., & Kaghazchi, P. (2015). Stabilization of the ?? -Sn phase in tin nanoparticles and nanowires. *Applied Physics Letters*, 107(12), 1–4. <https://doi.org/10.1063/1.4931353>
- Jo, Y. H., Park, J. C., Bang, J. U., Song, H., & Lee, H. M. (2011). New Synthesis Approach for Low Temperature Bimetallic Nanoparticles: Size and Composition Controlled Sn–Cu Nanoparticles. *Journal of Nanoscience and Nanotechnology*, 11(2), 1037–1041. <https://doi.org/10.1166/jnn.2011.3052>
- Kraynov, A., & Müller, T. E. (2011). Concepts for the Stabilization of Metal Nanoparticles in Ionic Liquids. In S. Handy (Ed.), *Applications of Ionic Liquids in Science and Technology*.
- Lai, B. R., Lin, L. Y., Xiao, B. C., & Chen, Y. S. (2019). Facile synthesis of bismuth vanadate/bismuth oxide heterojunction for enhancing visible light-responsive photoelectrochemical performance. *Journal of the Taiwan Institute of Chemical Engineers*, 100, 178–185. <https://doi.org/10.1016/j.jtice.2019.04.020>
- Maldonado, K. Luna, G. et al. (2017). Preparación y Caracterización de Nanocompositos Quitosano-Cobre con Actividad Antibacteriana para aplicaciones en Ingeniería de Tejidos. *Revista Mexicana de Ingeniería Biomedica*, 38(1), 306–313.
- Peponi, L., Puglia, D., Torre, L., Valentini, L., & Kenny, J. M. (2014). Processing of nanostructured polymers and advanced polymeric based nanocomposites. *Materials Science and Engineering R: Reports*, 85(1), 1–46. <https://doi.org/10.1016/j.mser.2014.08.002>
- Reverberi, A. P., Voccianta, M., Salerno, M., Caratto, V., & Fabiano, B. (2019). Bi nanoparticles synthesis by a bottom-up wet chemical process. *Chemical Engineering Transactions*, 73(July 2018), 283–288. <https://doi.org/10.3303/CET1973048>
- Rozenberg, B. a., & Tenne, R. (2008). Polymer-assisted fabrication of nanoparticles and nanocomposites. *Progress in Polymer Science*, 33(1), 40–112. <https://doi.org/10.1016/j.progpolymsci.2007.07.004>
- Sandra, S. C., Carapuça, H. M., & Duarte, A. C. (2005). Ion-exchange and permselectivity properties of poly(sodium 4-styrenesulfonate) coatings on glassy carbon: Application in the modification of mercury film electrodes for the direct voltammetric analysis of trace metals in estuarine waters. *Talanta*, 65(3), 644–653. <https://doi.org/10.1016/j.talanta.2004.07.032>
- Serrano, N., Alberich, A., Díaz-Cruz, J. M., Ariño, C., & Esteban, M. (2008). Signal splitting in the stripping analysis of heavy metals using bismuth film electrodes: Influence of concentration range and deposition parameters. *Electrochimica Acta*, 53(22), 6616–6622. <https://doi.org/10.1016/j.electacta.2008.04.055>
- Shrivastava, S., Jadon, N., & Jain, R. (2016). Next-generation polymer nanocomposite-based electrochemical sensors and biosensors: A review. *TrAC - Trends in Analytical Chemistry*, 82, 55–67. <https://doi.org/10.1016/j.trac.2016.04.005>
- Suarez, O. (2017). *Obtención y caracterización electroquímica y estructural de nanocompositos de copolímeros sulfonados/bismuto – estaño*. Universidad Nacional de Colombia.
- Suarez, O., Olaya, J. J., & Mendoza, M. (2018). Electrochemical and structural characterization of Nafion/Bismuth-Tin nanocomposites stabilized with polyoxyethylene 23 lauryl ether (Brij). *Materials Chemistry and Physics*, 207, 499–506. <https://doi.org/10.1016/j.matchemphys.2017.12.067>
- Wei Ni, Jianli Cheng, L. S. et al. (2012). Integration of Sn/C Yolk-Shell Nanostructures into Free-standing Conductive Networks as Hierarchical Composite 3D Electrodes and the Li-ion Insertion/ Extraction Properties in a Gel-type Lithium-ion Battery Thereof. *Journal of Materials Chemistry A*, 1. <https://doi.org/10.1039/x0xx00000x>